# STUDIES OF CONTROLLED LASER-INDUCED MICROBUNCHING INSTABILITY AT SOURCE DEVELOPMENT LABORATORY *

S. Seletskiy#, B. Podobedov, Y. Shen, X. Yang, National Synchrotron Light Source, Brookhaven National Laboratory, Upton, NY 11973, U.S.A.

*Abstract*

We present the studies of controlled microbunching intentionally induced on the beam by the photocathode laser with modulated longitudinal profile. Varying the depth and frequency of longitudinal modulation of the laser pulse allowed us to observe the development of microbunching instability at BNL Source Development Laboratory (SDL) in the controlled environment. That allowed us to benchmark the model of the microbunching gain for the first time. In addition to that, we demonstrated for the first time a constructive work of a so-called longitudinal space charge amplifier, which in case under consideration can be utilized for enhancement of linac-based sources of THz radiation.

## INTRODUCTION

A linear accelerator with a bunch compressor (BC) can amplify the initial small modulation in electron beam longitudinal density, leading to microbunching instability [1-4].

The microbunching instability was observed and experimentally characterized [5] at the SDL [6] and other facilities, and mitigation of microbunching instability with so-called laser heater [7] was demonstrated at SLAC Linac Coherent Light Source [8]. It was shown [5,9] that the main driver of the instability is the Longitudinal Space Charge (LSC) wakefield. Both the shot noise and the initial longitudinal modulations of the photocathode laser can be the initial source of microbunching. In spite of the success in understanding and controlling the microbunching instability the direct benchmarking of the model for microbunching gain is still missing.

Here we report the studies that allowed us to perform such benchmarking. We induced the initial microbunching on the electron beam at several wavelengths and amplitudes by introducing respective longitudinal modulation into the photocathode laser. Measuring and comparing the depth of modulation for the compressed and uncompressed beam we directly measured the microbunching gain at respective wavelengths.

Additionally, the microbunching instability developing in typical linacs with the BC can be considered as a longitudinal space charge amplifier (LSCA) with a large relative bandwidth, typically in the range of 50%-100%. It was suggested [10] to use such amplifier for generation of vacuum ultraviolet (VUV) and x-ray radiation. Curiously, our experiment gives a proof of principle demonstration of the LSCA concept and suggests that LSCA can be applied to increasing the tunability of the linac-based THz sources [11].

## EXPERIMENTAL SETUP

In SDL the electron beam generated in photocathode RF gun is accelerated to 70 MeV, and compressed in the bunch compressor (BC) consisting of the linac section, which introduces correlated energy spread, and the four-bend chicane. The BC is followed by three linac sections capable of accelerating electron beam up to 300 MeV. Fully accelerated beam is fed to the 10 m long undulator to produce coherent radiation from IR to XUV. The SDL beamline is equipped with a spectrometer magnet located downstream of the BC, followed by a beam profile monitor (BPM). The SDL layout is schematically shown in Figure 1.

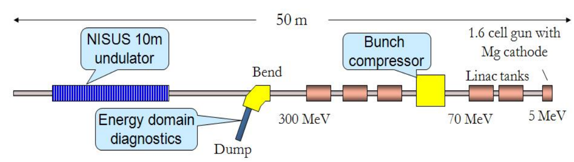


Figure 1: The SDL layout.

The photocathode RF gun is illuminated by a frequency tripled Ti:sapphire laser at 265 nm. The SDL Ti:sa laser system consists of a 100 fs RF synchronized oscillator and a chirped pulse amplifier. To produce a tuneable longitudinally modulated laser pulse used in our experiment the chirped 265 nm laser pulse is split into two pulses by a 50/50 beam splitter, and one pulse is delayed by a variable interval $\tau$ with respect to the other. The two chirped pulses are then recombined. The time difference between these two pulses produces a beat frequency $2b\tau$ that is directly proportional to the time delay $\tau$ and the frequency chirp rate $b$. The resultant output pulse has a Gaussian envelope modulated by a cosine function with a center frequency of $2b\tau$, which can be easily tuned by varying the time delay or the frequency chirp of the input pulses.

The electron beam energy spectrometer located downstream of the fifth linac tank can be utilized to obtain beam temporal profile as well as its energy spectrum. For the former one can use RF zero phasing method. The electron beam is energy chirped by one of the linac sections set to the nonaccelerating (zero) phase, and then it is dispersed by a dipole magnet, so that the different time slices of the beam are projected on the scintillating screen at different positions. This method gives the RMS time resolution of 7 fs [5].

*Work supported by US Department of Energy, Contract DE-AC02-98CH1-886.
#seletskiy@bnl.gov

Copyright © 2012 by IEEE — cc Creative Commons Attribution 3.0 (CC BY 3.0) — cc Creative Commons Attribution 3.0 (CC BY 3.0)

## DIRECT MEASUREMENT OF MICROBUNCHING GAIN

The LSC wakefield upstream of the bunch compressor converts small beam density modulation at the beginning of a linac into energy modulation. The energy modulation of amplitude $\Delta\gamma$ prior to BC is converted into additional density modulation due to nonzero dispersion in the BC, thus giving a rise to microbunching instability. The microbunching gain factor is [3]:

$$G = \left| CkR_{56} \frac{\Delta\gamma}{\gamma b(k)} \right| \exp\left( -\frac{(CkR_{56}\sigma_\gamma/\gamma)^2}{2} \right) \quad (1)$$

where $C$ is compression ratio, $k$ is modulation wavenumber, $R_{56}$ is momentum compaction, $b(k)$ is bunching factor characterizing beam density modulation, $\gamma$ is relativistic gamma factor and $\sigma_\gamma$ is the rms energy spread.

The change in the energy modulation along the linac due to the longitudinal space charge (LSC) wake $Z(k,z)$ is:

$$\Delta\gamma(k,s) = -\frac{4\pi I}{Z_0 I_A} \int_0^s Z(k,z) b(k,z) dz \quad (2)$$

Here $I$ is beam current, $Z_0$=377 Ω is the free-space impedance and $I_A$=17 kA is Alfven current.

To perform the direct measurement of the microbunching gain we compare the modulation amplitude of the uncompressed beam modulated in density by the photocathode laser with the modulation amplitude of the compressed beam. The example of the electron beam produced by the longitudinally modulated photocathode laser is given in Fig. 2. The zero phasing measurement of this 90 pC beam shows that its length is 3 ps FWHM and the induced modulation wavelength is 60 µm. According to equation (1) we can expect to see microbunching amplification at wavelengths $\lambda \geq 30$ µm for such beams at the BC compression factor of 2-3.

We compress the modulated electron beam and then perform zero phasing measurement with accelerating section 4 after removing the residual energy chirp with section 3. Since the modulation of only 2-3% can be resolved on the spectrometer screen the maximum gain that one can reliably measure at SDL is not higher than ≈40. This sets the limit on the BC compression ratio one can use in the experiment. In our studies we chose compression of 2.5.

The zero phasing measurement performed for the compressed 90 pC beam from Fig. 1 is shown in Fig. 3. In accordance with the theory, the microbunching instability dramatically increases the modulation of compressed beam.

The described measurement was performed at several wavelengths. For each wavelength a camera images of the beam were saved for several shots. At the present time we are working on the systematic of the proper background subtraction and accounting for the shot-by-shot variation in beam amplitudes. The preliminary results are shown in Fig. 4.

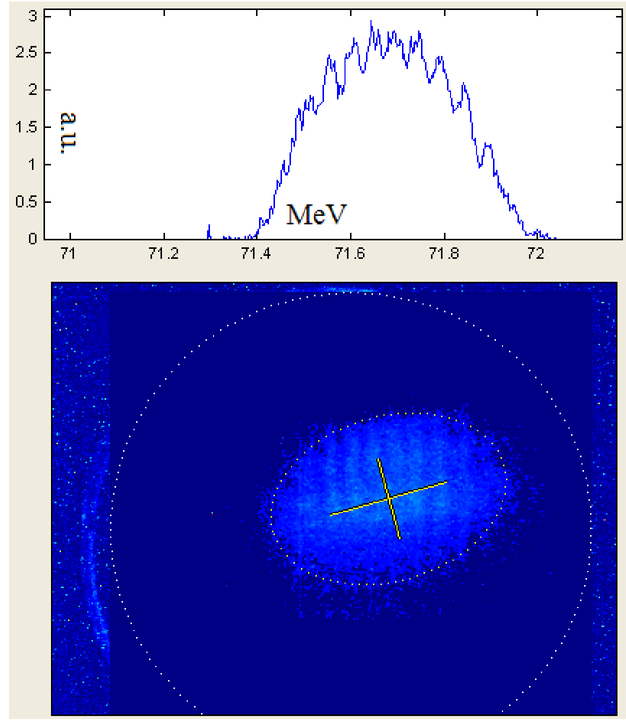


Figure 2: Zero phasing measurement of the 90 pC, 3 ps (FWHM) long electron beam produced by the longitudinally modulated photocathode laser. The wavelength of the induced modulation is 60 µm.

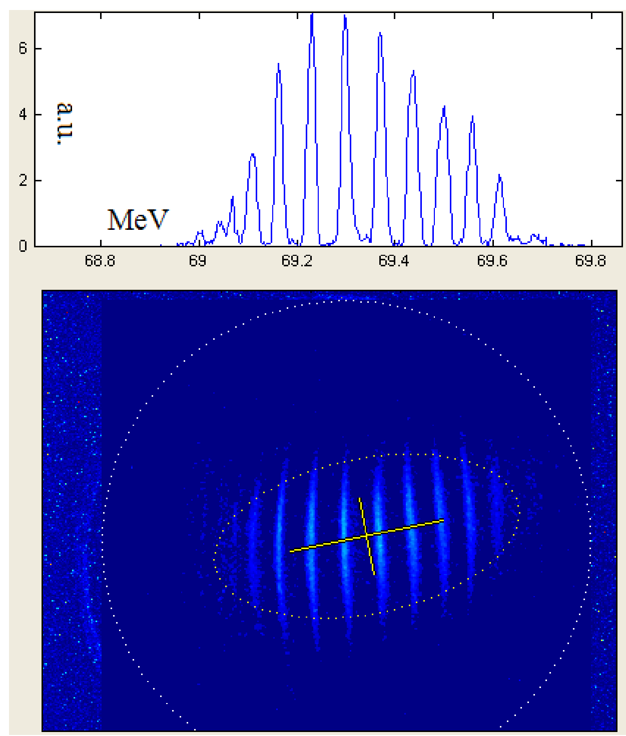


Figure 3: The zero phasing of the compressed 90 pC beam. The BC compression factor is 2.5.

As one can see, the good quantitative correspondence between the experiment and the theory is observed for the

Copyright © 2012 by IEEE – cc Creative Commons Attribution 3.0 (CC BY 3.0) — cc Creative Commons Attribution 3.0 (CC BY 3.0)


ISBN 978-3-95450-115-1

wavelengths of up to 170 µm. For longer wavelengths the correspondence between the theory and experiment is only qualitative. The reason for that is not understood yet. At 220 µm $k\sigma_z = 17$, which still is within the limits of theory applicability ($k\sigma_z >> 1$).

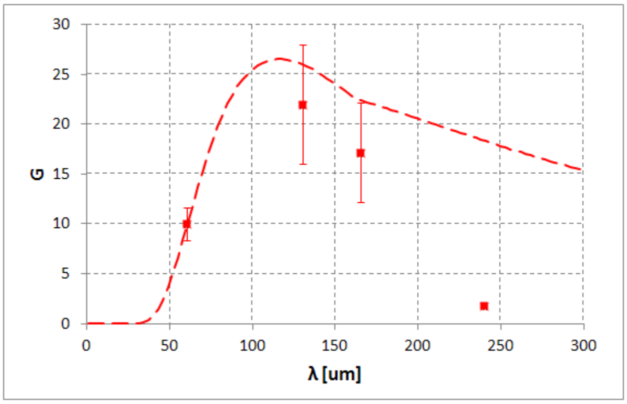


Figure 4: Comparison of the direct measurement of microbunching gain (dots) and the theoretical predictions (line). Horizontal axis shows modulation wavelength of the uncompressed beam. The vertical axis shows microbunching gain.

## LSC AMPLIFIER FOR LINAC-BASED THZ SOURCE

The LSC amplifier suggested in [10] starts from the shot noise and generates radiation in VUV and x-ray ranges. Such amplifier can be an addition to some existing or planned free electron lasers helping to extend the operating range towards longer wavelength.

Our studies present a first proof of principle experiment that demonstrates the operation of the LSCA of a slightly different type. We start the LSCA from the coherently seeded density modulation obtained from longitudinally modulated photocathode laser pulse. The wavelengths of considered modulation are of interest for the THz sources. Therefore, we suggest that the demonstrated LSCA can be applied to increase the tunability of the linac-based THz sources.

Indeed, a linac equipped the longitudinally modulated photocathode laser described above can serve as a source of tuneable, narrow-band, few-cycle and multicycle coherent THz radiation [11]. Although higher charge per bunch is desired for strong THz radiation, the charge and modulation frequency of the electron beam utilized in the considered THz source, and therefore the tunability of such source, are fundamentally limited by the space charge effects at low energy. As the bunch charge or the modulation frequency increase, the density modulation of electron beam is washout because the phase space of each electron sub-bunch grows, leading to the overlap of adjacent bunches. The maximum charge and modulation wavelength achievable in this method are about 100 pC and ~115 µm respectively [11].

Our experiment clearly demonstrates that the application of the LSCA overcomes this limitation. For instance, the 90 pC beam shown in figure 3 is modulated at 23 µm wavelength.

We were also able to break the charge limit. As an example, we obtained the 250 pC beam modulated at 40 µm.

## CONCLUSION

In this paper we performed a set of controlled microbunching measurements at the SDL facility at BNL.

We induced the longitudinal density modulation upon the electron beam by prompting it from the photocathode with respect to the longitudinally modulated laser pulse.

Comparison of the depth of modulation of the compressed and uncompressed electron beams allowed us to perform the benchmarking of theoretical calculations of the gain of microbunching instability for the first time. The good quantitative agreement between the experiment and theory was observed.

We also performed a proof of principle experiment demonstrating the application of the longitudinal space charge amplifier to the tuneable linac-based source of THz radiation. Our results significantly broaden the scope of operation of such THz sources.

## ACKNOWLEDGEMENTS

We are grateful for support from the NSLS. This work is supported in part by the U.S. Department of Energy (DOE) under contract No. DE-AC02-98CH1-886.

## REFERENCES

[1] M. Borland et al., Nucl. Instrum. Methods Phys. Res., Sect. A 483, 268 (2002).
[2] Z. Huang and K. Kim, Phys. Rev. ST Accel. Beams 5, 074401 (2002).
[3] E. Saldin, E. Schneidmiller and M. Yurkov, Nucl. Instrum. Methods Phys. Res., Sect. A 483, 516 (2002).
[4] S. Heifets, S. Krinsky and G. Stupakov, Phys.Rev. ST Accel. Beams 5, 064401 (2002).
[5] S. Seletskiy et al., Phys. Rev. ST Accel. Beams 14, 110701 (2011).
[6] J.B. Murphy and X.J. Wang, "Laser-Seeded Free-Electron Lasers at the NSLS", SRN, Vol. 21, No. 1, 41, 2008.
[7] E. Saldin, E. Schneidmiller, and M. Yurkov, Nucl. Instrum. Meth. A 528, 355 (2004).
[8] Z. Huang et al., Phys. Rev. ST Accel. Beams 13, 020703 (2010).
[9] T. Shaftan, Z. Huang, Phys.Rev. ST Accel. Beams 7, 080702 (2004).
[10] M. Dohlus et al., Phys. Rev. ST Accel. Beams 14, 090702 (2011).
[11] Y. Shen et al., Phys. Rev. Lett. 107, 204801 (2011).

Copyright © 2012 by IEEE – cc Creative Commons Attribution 3.0 (CC BY 3.0) — cc Creative Commons Attribution 3.0 (CC BY 3.0)